PHYSICAL REVIEW B VOLUME 36, NUMBER 10 1 OCTOBER 1987

Size and location of the largest current in a random resistor network

Y. S. Li and P. M. Duxbury
Department of Physics and Astronomy and Center for Fundamental Materials Research, Michigan State University, East Lansing, Michigan 48824-1116
(Received 6 May 1987)

The largest current in the bonds of a random resistor network (RRN) is shown to have an anomalous size dependence given by $I_{\max} \sim (\ln L)^{\alpha}$, for L (the linear dimension of the network) $\gg \xi_p$ (the percolation correlation length). A second important current scale is the one that leads to the eventual failure of the RRN when it is considered to be a network of fuses. This second current is defined to be I_{com} and scales as $I_{\text{com}} \sim (\ln L)^{\beta}$. Analytic arguments are presented to support the inequality $1/[2(D-1)] \lesssim \beta \leq \alpha \lesssim 1$, where D is the spatial dimension. Numerical simulations in two dimensions support this, and in addition show that the bond carrying $I_{\max}$ is often near the free surfaces of the RRN. This statement is quantified by the ratio of surface to bulk probabilities, and this ratio is shown to increase algebraically with exponent $x = 0.30 \pm 0.05$ in two dimensions.

I. INTRODUCTION

The random resistor network is a paradigm for the study of transport in random media.[1] Recently, it has been extended to the study of breakdown in random media,[2–4] where it provides a nontrivial starting point in the study of crack initiation due to defects, and a simple starting point for the study of breakdown in quenched random media. In breakdown, the weakest part of the network fails first, and the effects of quenched defects are markedly more pronounced than in transport phenomena.[3,4] The origin of the strong effects of defects in breakdown problems is the dominance of extreme fluctuations in the microscopic load distribution in problems of this sort. In contrast, transport and elastic coefficients are related to the lower (typically the second) moments, of these microscopic load distributions (e.g., for the random resistor network, resistance is related to the second moment of the distribution of bond currents). Thus a study of breakdown involves new physical concepts and theoretical methods as well as being of great technological importance.

An analytic study of breakdown networks centers on the bonds carrying the largest loads, and in the case of the fuse network, the bond carrying the largest current. In a previous paper,[4] we have performed a detailed analysis of the physics of breakdown networks using the results of this paper, namely the fact that the largest bond current in a random resistor network (RRN) with p present bonds of resistance 1 Ω, and $1-p$ vacant bonds, scales with L, the linear dimension of the network, as

$$I_{\max} \sim (\ln L)^{\alpha} , \tag{1}$$

$$I_{\text{com}} \sim (\ln L)^{\beta} , \tag{2}$$

for L (the linear dimension of the network) $\gg \xi_p$ (the percolation correlation length). $I_{\max}$ is the largest current in the random resistor network, and I_{com} is the largest current in a failure initiating bond (to be defined in Sec. II). α and β are enhancement exponents. In Sec. II we use analytic arguments to support Eqs. (1) and (2), and to suggest that α and β obey the approximate inequality

$$1/[2(D-1)] \lesssim \beta \leq \alpha \lesssim 1 , \tag{3}$$

where D is the spatial dimension. A two-crack calculation supports the equality $\alpha = 1$ in two dimensions. In our earlier letter studying size effects in breakdown networks,[3] we used the approximation $\alpha = \beta = 1/(D-1)$, based on the current density at the ends of elliptical defects. This result certainly lies within the bounds given in Eq. (3) above, and also agrees with the two-dimensional results presented in this paper. There has also been some recent work on the random resistor network with two nonzero conductivities by Machta and Guyer.[5] They show that funnel defects are the dominant single defects in that problem, and define enhancement exponents that turn out to be dependent on the ratio of the two conductivities.

Numerical simulations are used in Sec. III to test the analytic predictions for the two-dimensional random resistor network. In addition, we study the *location* of the largest current in the network and find that in a system with free boundary conditions, there is a strongly enhanced probability near the free surfaces of the network. Translated into breakdown language, this implies that cracks are often initiated near the surfaces of a sample. The paper concludes in Sec. IV.

II. ANALYTIC STUDY

In the dilute limit, where $L \gg \xi_p$, defect clusters are well separated, and may, in a first approximation, be treated independently. We consider L^d random resistor (1 Ω per present bond) networks that have a current of 1 A through each vertical bond in the pure limit. Upon adding a small fraction $1-p$ of defects (which have zero conductivity), we then wish to find the size of the current in the hottest bond (the bond carrying the largest current). In two dimensions, long thin defects are especially efficient at causing current enhancements near their ends [see Fig. 1(a)], and our analysis begins by calculating the current enhancements due to defects of this sort. The largest defects of this sort have the largest current enhancements, and as we have shown previously,[3,4] the largest defects of this form are of size $\ln L$. To find the current at the end of a defect like that shown in Fig. 1(a) on the lattice, we use the continuum approximation shown in Fig. 1(b). The solution to this problem in two dimensions may be found using elliptical coordinate solutions to Laplace's equations, and is given in our previous paper,[4] from which we take the result

$$j_{\text{tip}}(x)=j_\infty\left[1+\frac{\cosh\xi_a \exp(\xi_a-\xi)}{\sinh\xi}\right], \tag{4}$$

where $j_{\text{tip}}(x)$ is the current density at distance x from the tip (at $x=a$) of the defect along the $y=0$ axis, $\xi=\cosh^{-1}(x/c)$, and j_∞ is the current density a large distance away from the defect. To find the prediction that this result makes in the lattice problem, we must integrate over the lattice spacing d, to find

$$\begin{aligned} I_{\text{tip}} &= \int_a^{a+d} j_{\text{tip}}(x)dx \\ &= \int_{\xi(a)}^{\xi(a+d)} j_\infty\left[1+\frac{\cosh\xi_a \exp(\xi_a-\xi)}{\sinh\xi}\right] c\sinh\xi d\xi \\ &= I_\infty\left[1+\frac{a}{d}[1-\exp(\xi_a-\xi_{a+d})]\right], \end{aligned} \tag{5}$$

where $\xi_a=\cosh^{-1}(a/c)$, $\xi_{a+d}=\cosh^{-1}[(a+d)/c]$, and $I_\infty=j_\infty d$ is the current flowing in a vertical bond a long way from the defect. In the majority of this paper we take $I_\infty=1$. In terms of d, a, and b, there are two limiting behaviors in I_{tip},

$$\text{(i) } da \ll b^2 \quad \text{where } I_{\text{tip}} \sim I_\infty(1+a/b) \tag{6}$$

and

$$\text{(ii) } da \gg b^2 \quad \text{where } I_{\text{tip}} \sim I_\infty(1+\sqrt{2a/d}\,)\ . \tag{7}$$

For an L^D (D is the spatial dimension) RRN, the lattice spacing $d=1$. In addition, b corresponds the thickness of the long thin defect of Fig. 1(a) in the y direction, and so $b=1$. Since $a\sim\ln L$, the limit $da\gg b^2$ is the correct limit to take in comparing the ellipse result with the lattice problem. Using the single-ellipse result, one then finds that somewhere in the RRN there is a bond whose current scales as

$$I_{\text{2D ellipse}} \sim (\ln L)^{1/2}\ . \tag{8}$$

Now consider the random resistor network to be a breakdown network by changing all of the resistors to 1-Ω, 1-A fuses. The failure of the bond at the end of an "ellipselike" defect will lead to the eventual failure of the whole network, as the crack grows from the outer tips of the long thin defect in Fig. 1(a). The ellipse thus gives

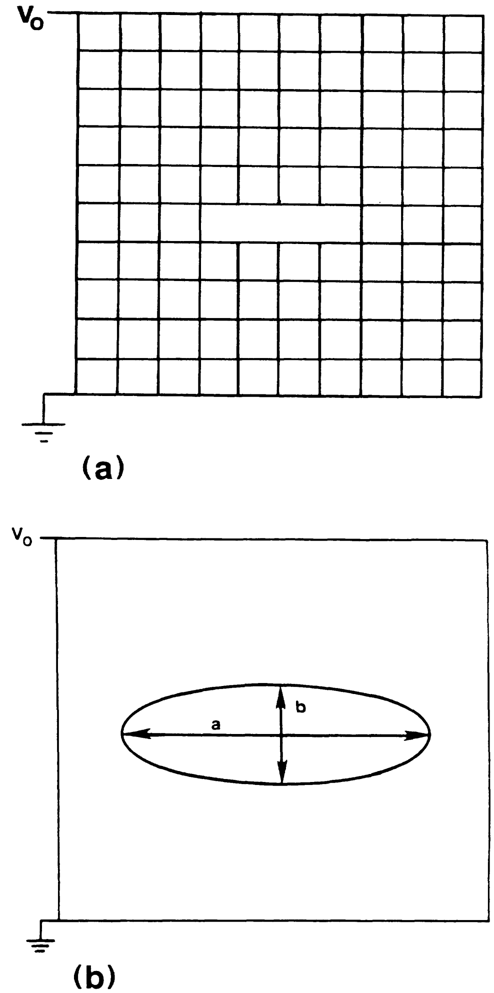

FIG. 1. (a) A failure-inducing single defect in the square-lattice random resistor network. (b) An elliptical defect that acts as a continuum-limit representation of the defect in (a).

an estimate of the current in a "failure-initiating" bond, and from it we obtain the estimate $I_{\text{com}} \geq I_{\text{ellipse}}$. There are, however, defect configurations that lead to large current enhancement and do not lead to the failure of the whole network. One such configuration is shown in Fig. 2(a). The bond in the middle of the two cracks in this figure carries the most current. However, when it fails it does not necessarily lead to the eventual failure of the whole network.[5] This sort of crack configuration is considered further below. Before doing this, we find I_{com} in three dimensions based on calculations using a oblate spheroidal defect found by forming a solid of revolution about the y axis of Fig. 1(b). Solving Laplace's equations in oblate spheroidal coordinates,[6] one finds, for the current density as a function of distance from the edge of the $y=0$, $r=a$ circle,

$$j_y=j_\infty\{1-[\cot^{-1}(\sinh u)-(\sinh u)^{-1}]/[\cot^{-1}(\sinh u_0)-\sinh u_0/(1\sinh^2 u_0)]\}\ , \tag{9}$$

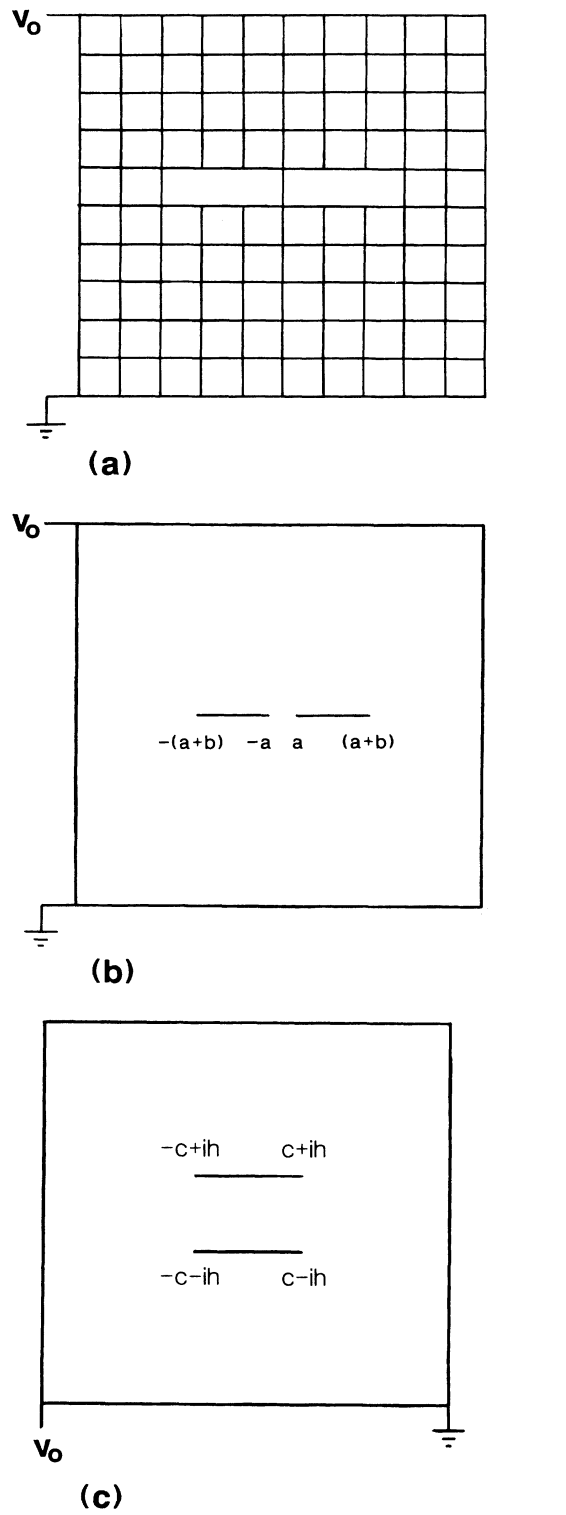

FIG. 2. (a) A strong current-enhancing defect configuration in the square-lattice RRN. The bond between the two defects carries a large current (see text). (b) A continuum representation of the defect in (a). The defects are infinitesimal slits lying along the x axis. (c) Under a conformal transformation, the defect configuration of (b) is transformed to that shown in this figure. The calculation of the electric field in this geometry is trivial.

where $a=c\cosh u_0$, $r=(x^2+z^2)^{1/2}=c\cosh u$, $b=c\sinh u_0$, and $a^2=b^2+c^2$. This is integrated over the lattice spacing d in the x and z directions, and again taking the limit $da \gg b^2$, with $b \sim d$ to obtain the lattice limit, we find

$$I_{\text{tip}} \sim I_\infty 2^{3/2}/\pi(a/d)^{1/2} , \tag{10}$$

with the result $a \sim n_{\max}^{1/2} \sim (\ln L)^{1/2}$ in three dimensions (3D),[3,4] and we find, further,

$$I_{\text{com}} \geq (\ln L)^{1/4} \quad (\text{in 3D}) . \tag{11}$$

Again this defect leads to the eventual failure of the whole network as the crack grows from the outer edges of the "penny-shaped" crack. Combining the equations above for I_{com} in two and three dimensions, we find

$$I_{\text{com}} \sim (\ln L)^{\beta} \quad \text{with } \beta \geq 1/[2(D-1)] . \tag{12}$$

Here we have written $\beta \geq 1/[2(D-1)]$ because although the isolated ellipse and spheroidal defects that we have studied will certainly lead to failure of the network, there may be other configurations that we have not studied that lead to failure more readily. The ellipse result thus provides an approximate lower bound on β. It is only an approximate lower bound, as we cannot rigorously exclude the possibility that the network may be stronger than the prediction found from the ellipse result; although on physical grounds we consider it unlikely, and the numerical evidence[3,4] (also see Sec. III) supports Eq. (12).

It is straightforward to find a defect configuration that leads to a greater current enhancement than that induced by the ellipse. In two dimensions, one such defect is shown in Fig. 2(a). The bond between the two cracks carries the most current, and we can make an analytic estimate of its current by solving a continuum two-crack problem. It is not possible to solve the two-ellipse problem, but it is possible to solve the problem of two infinitesimal slits in two dimensions by using conformal transformation techniques. We thus replace the lattice problem of Fig. 2(a) by the continuum problem of Fig. 2(b). By conformal transformation, the two-slit problem of Fig. 2(b) is transformed as depicted in Fig. 2(c), a problem that is trivially solvable for infinitesimally thin slits. The form of the conformal transform is quite complex, however, so we defer detailed calculations to the Appendix. The current density between the two slits of Fig. 2(b) [Eq. (A26)] is then integrated over the lattice spacing d, to find, for the current between the two slits in the lattice limit [Eq. (A30)],

$$I_{\text{slits}} = 2j_\infty(a+b)[E(k)-K(k)+E(k')K(k)/K(k')] , \tag{13}$$

where $2a$ is the distance between the two cracks [see Fig. 2(b)], b is the length of each crack, $k=a/(a+b)$, $k'=[(1-k^2)]^{1/2}$, and $K(k)$ and $E(k)$ are, respectively, elliptic integrals of the first and second kind. When the cracks are close so that $a/b \to 0$ and $k \to 0$, we find

$$I_{\text{total}} \sim (a+b)/\ln[(a+b)/a] , \tag{14}$$

which implies

$$I_{\max} \sim \ln(L)/\ln[\ln(L)] \; , \tag{15}$$

or $\alpha=1$, ignoring the $\ln[\ln(L)]$ correction. As a technical aside, it is interesting to note that although the single-slit result does not produce the same current density at the slit tip as is found at the ellipse tip, after integrating over the lattice spacing the ellipse and the slit give the same expression for the current (this is demonstrated in the Appendix).

In general, we believe that it is always possible to find a defect configuration that channels a current proportional to the defect size through one critical conducting bond, and hence that $\alpha=1$ for any dimension. In any case, $\alpha=1$ is an upper bound on the amount of current that can be channeled by an isolated defect cluster, just due to current conservation. Based on the isolated defect cluster calculations described above and Eq. (12), we thus find the approximate inequality given in the Introduction [Eq. (3)],

$$1/[2(D-1)] \lesssim \beta \lesssim \alpha \lesssim 1 \; . \tag{16}$$

The only way that this result can be invalidated is for the cumulative effects of many defect clusters to lead to qualitatively new behavior. We may estimate the maximum enhancement this effect may have by replacing each defect cluster by a dipole current source, and considering a random distribution of such dipoles on the lattice. The maximum cummulative effect of such a distribution of dipoles is

$$I_{\max} \sim \int_1^L dr\, r^{D-1}(1-p) I_{\text{dipole}}/r^D \; , \tag{17}$$

where I_{dipole} is the average strength of one dipole [$O(1)$ for $L \gg \xi_p$]. The integrand is the maximum contribution to a bond current at the origin due to all dipoles on the hypersphere at distance r. Upon doing the integral, one finds

$$I_{\max} \sim \ln L \quad \text{in all dimensions} \; . \tag{18}$$

The failure of such a bond does not necessarily lead to the failure of the network, and the long-range cummulative effects of dipole current sources thus lead to the prediction $\alpha \leq 1$ as found above using defect-cluster arguments. We thus believe that Eq. (16) provides reliable bounds on α and β, and that the evidence is quite strong that $\alpha=1$ in two dimensions. In the next section we test the analytic predictions that we have made above by doing numerical simulations on the two-dimensional random resistor network.

III. NUMERICAL SIMULATIONS

In order to test our predictions, we have performed numerical simulations on $L \times L$ square-lattice random resistor networks. As described in our previous paper,[4] we use the conjugate-gradient method to solve Kirchhoff's equations on this network. In the calculations described here, we apply an external current of 1 A per vertical bond and free boundary conditions in the transverse direction. The solution is considered to have converged adequately when the residual vector[4] is less than 1.0×10^{-7}.

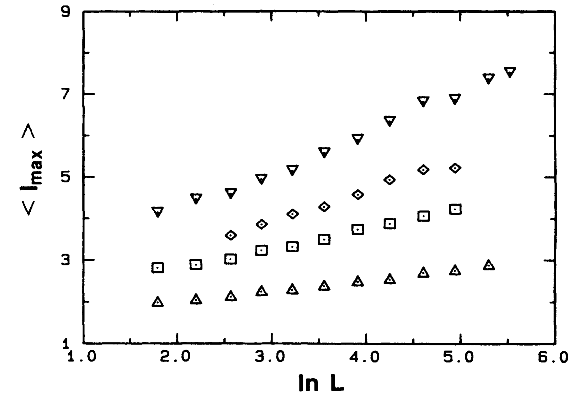

FIG. 3. The size of the largest bond current, $\langle I_{\max} \rangle$, on $L \times L$ square lattice random resistor networks as a function of the lattice size L, for $p=0.90$ ($\triangle$), $p=0.80$ ($\square$), $p=0.75$ ($\Diamond$), and $p=0.70$ (∇). Each point is an average over 50 realizations.

In Fig. 3 we plot the maximum current $I_{\max}$ (averaged over 50 realization) as a function of lattice size L, with L ranging from 10 to 200 for several values of p. At all values of p presented in the figure, the data suggest that $I_{\max}$ is linearly dependent on $\ln L$, and hence that $\alpha=1$ in two dimensions. These numerical data thus support the prediction found from the analytic arguments of the preceding section, and we thus believe $\alpha=1$ in two dimensions for $L \gg \xi_p$.

As discussed previously,[3,4] $I_{\text{com}} = I_{\max}$ when there are no defects in the system, and also that $I_{\text{com}} \sim I_{\max}$ at the percolation point. We thus have chosen to do a detailed comparison of I_{com} with $I_{\max}$ at $p=0.75$, as any differences between these two quantities should be noticable at this defect fraction. It is much more time consuming computationally to calculate I_{com} as it involves carrying the crack-propagation process to completion. The data presented in Fig. 4 on square lattices of sizes

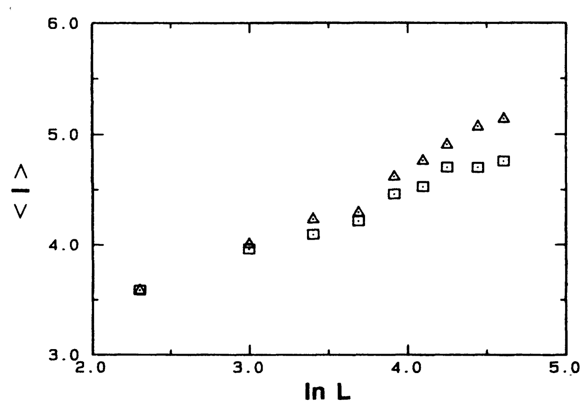

FIG. 4. A comparison of the size of the bond currents, $\langle I_{\max} \rangle$ ($\triangle$) and $\langle I_{\text{com}} \rangle$ ($\square$), as a function L for $p=0.75$. Each point is an average over 50 realizations.

from $L=10$ to 100 with 50 realizations per lattice size took 5 h of CYBER 205 CPU time. The data are consistent with the equality $\alpha=\beta=1$ in two dimensions, although the $I_{\rm com}$ data have some downward curvature. The data are certainly consistent with the theoretical prediction given in Eq. (16) of the preceding section.

The prediction that $\alpha=1$ in two dimensions has implications for the nature of the tail of the bond-current distribution occurring in the RRN. The fact that the largest current increases logarithmically implies that the tail of the bond-current distribution is exponential, as can be seen from the following equation,

$$L^D \exp(-BI_{\max}) \sim 1 \ , \tag{19}$$

where B is independent of L, and so

$$I_{\max} \sim \ln L \ . \tag{20}$$

The relationship between the extreme values of a distribution and the nature of the distribution tail is well studied in statistics, and may be found, for example, in the book by Gumbel.[8] Another numerical test of the exponent α is thus to study the form of the tail of the distribution of bond currents. The bond-current distribution for $L=80$ square networks with $p=0.80$ and 0.90 is shown in Fig. 5(a). The two-peak structure of the distribution in Fig. 5(a) is a reflection of the fact that when there are no defects in the network, the vertical bonds all carry the same current, while the horizontal ones carry none. In the pure limit the distribution function is thus two delta functions, one at the origin and one at a current of 1 A. This two-peak structure persists for defect fractions quite close to the percolation point. In this paper we are most interested in the tail of the distribution function, and, in particular, we expect the tail to be exponential in I, if the value $\alpha=1$ is correct in two dimensions. The bond-current distribution data in the tail of the distribution of Fig. 5(a) is plotted to fall on a straight line if the tail is exponential, and, to the accuracy of the numerical data, it does.

The location of the largest current in the RRN also shows an interesting behavior as a function of the distance from the free edges of the network. This is shown in Figs. 6(a) and 6(b) for $L=50$ and 90 RRN at

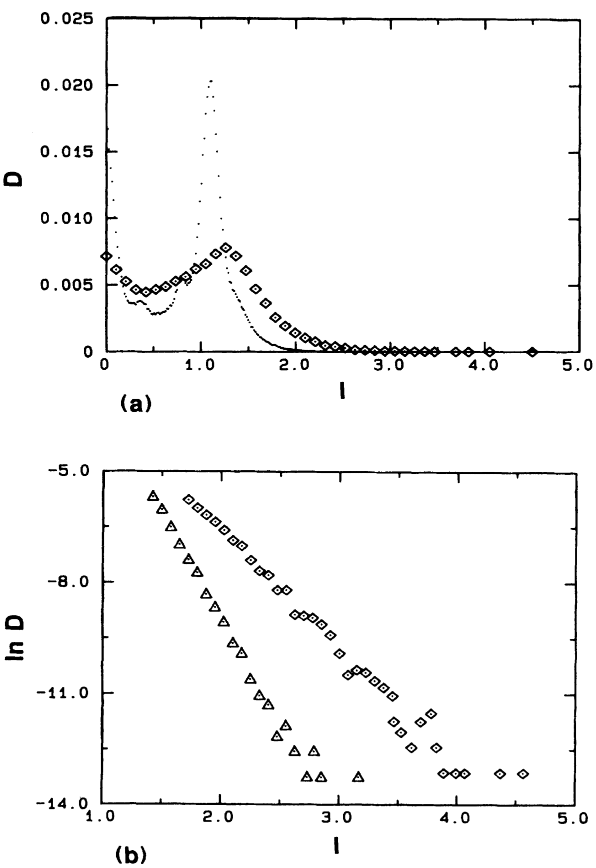

FIG. 5. (a) The probability distribution of bond currents for the square-lattice random resistor network for $p=0.90$ (●) and $p=0.80$ (◇). The figure was constructed from 50 realizations of an 80×80 square lattice. (b) The data of (a) plotted on a log-linear scale to emphasize the exponential tail of the distribution function. If the tail of (a) is exponential, we expect the tail in this figure to be linear.

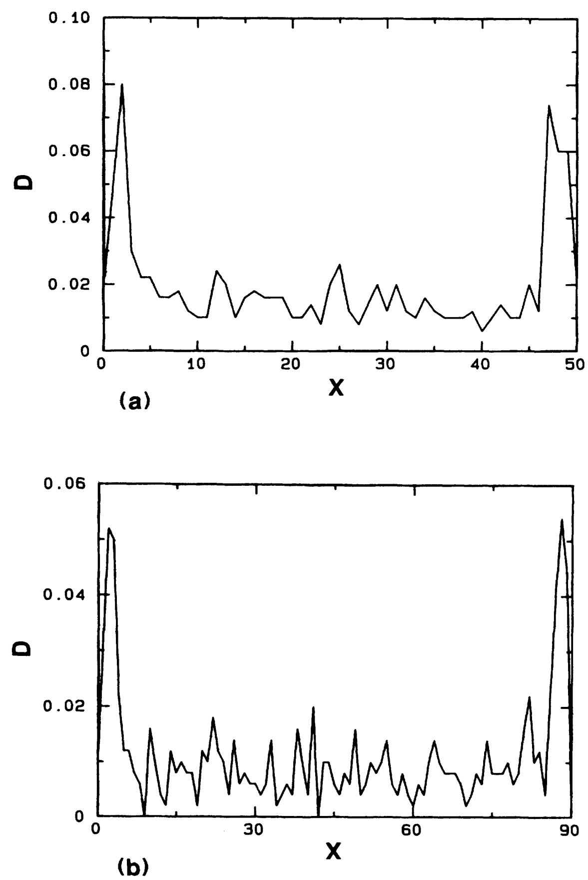

FIG. 6. The probability D that a bond distance x from one free surface of a square-lattice RRN carries the largest current in the network. The distribution function was constructed from 500 realizations of RRN's at $p=0.90$ for (a) $L=50$ and (b) $L=90$.

$p=0.90$. These figures show that there is a greatly enhanced probability of finding the bond with the largest current near the surfaces of the network. This may be quantified by measuring the ratio

$$R(L)=P_{\max}/P_{\text{bulk}} , \tag{21}$$

where, for $L=50$, $P_{\max}$ is the maximum of the curve in Fig. 6(a) and P_{bulk} is an average over the central region of the same graph. $R(L)$ appears to increase algebraicly with system size, as shown in Fig. 7, which implies that with increasing system size the probability that the bond carrying the largest current, lies near the surface, increases.

The results depicted in Figs. 6 and 7 may be qualitatively explained on the basis of isolated defect-cluster arguments. The effect is reflected in a isolated-defect problem, in the statement that as the isolated defect is moved closer to a free boundary the current at its tip increases markedly. A graphical representation of this effect is also given in Fig. 8 (rectangles), where the current at the tip of the defect of Fig. 1(a) is monitored, as the defect is moved towards the edge of the system. A similar effect occurs for the defect of Fig. 2(a), and is shown in Fig. 8 (triangles), where the current in the bond at the center of the two cracks in Fig. 2(a) is shown as a function of distance from the free edges of the network. From Fig. 8 it is seen that defects close to the free edges of the networks lead to greater current enhancements than the same defects in the bulk. An approximation to the enhanced surface probability is to frame the question in a slightly different way. Namely, what size surface defect do we need to have to produce the same current as a reference defect in the bulk? In the case of the defect of Fig. 2(a) the defect at the surface needs to be about $\frac{3}{4}$ (for an 80×80 lattice) the size of its bulk counterpart. On then finds for this type of defect cluster the following enhancement in finding the defect at the surface,

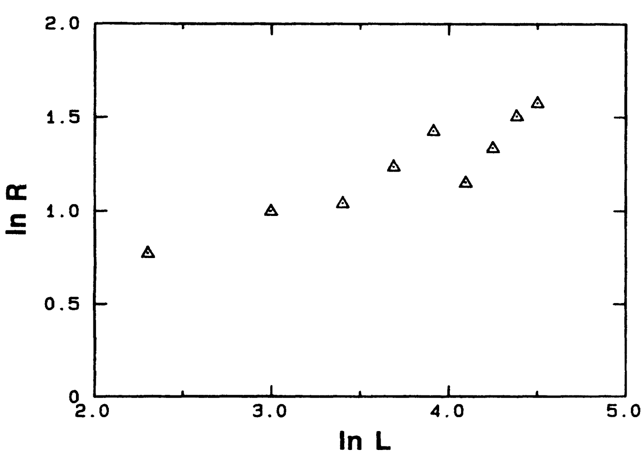

FIG. 7. A plot of the ratio of the maximum of Fig. 6 to the bulk average as a function of system size L, for L from 10 to 90 at $p=0.90$.

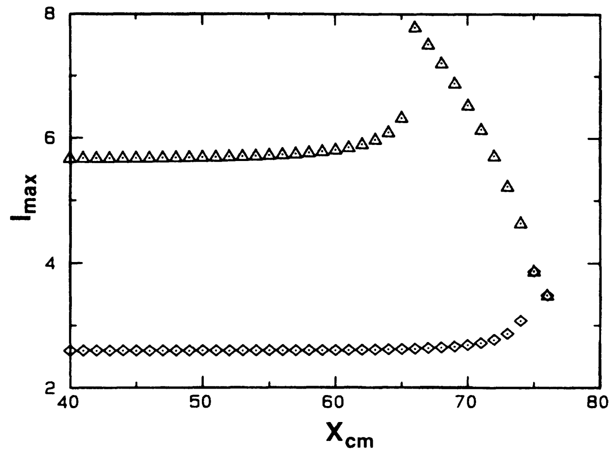

FIG. 8. The effect on $I_{\max}$ of moving the defect of Figs. 1(a) (◇) and 2(a) (△) towards the free surface of the RRN. The calculations were performed on an 80×80 lattice, with nine bond defects. X_{cm} measures the center of the isolated defect, and the figure gives the size of $I_{\max}$ as a function of X_{cm}.

$$R=P_{\text{surface}}/P_{\text{bulk}}$$
$$\sim(1-p)^{-3\ln L/4[\ln(1-p)]}/(1-p)^{-\ln L/\ln(1-p)} , \tag{22}$$

where we have used Eqs. (7) and (8) of Ref. 4 to derive (22). We then find

$$P_{\text{surface}}/P_{\text{bulk}}\sim L^{1/4} . \tag{23}$$

We expect that the qualitative behavior is correctly given by these arguments for general lattice dimensions and when the random distribution of defects is included into the network, but with a different exponent. From the results of simulations of the full network presented in Fig. 7, we find this surface probability exponent, x, to be (at $p=0.90$)

$$R=P_{\max}/P_{\text{bulk}}\sim L^{x} , \tag{24}$$

with

$$x=0.3\pm 0.05 . \tag{25}$$

Translated into breakdown language, the results of Eqs. (24) and (25) suggest that cracks are often initiated near the surfaces of the sample. This is an effect that is often observed in both electrical and mechanical breakdown situations, but is usually attributed to extra surface defects or surface inhomogenieties. Although these probabilities do often occur in real situations, the results discussed above show that the presence of a free surface is of itself enough to induce a greatly enhanced probability of crack initiation in its vicinity.

IV. CONCLUSIONS

In this paper we have studied the size and location of the largest current in a RRN. Our conclusions are as follows.

(1) The largest current in a RRN, with fraction $1-p$ of zero-conductivity bonds, on length scales $L\gg\xi_p$, has the scaling behavior $I_{\max}\sim(\ln L)^{\alpha}$, while the size of the

current in the failure-initiating bond has the scaling behavior $I_{\text{com}} \sim (\ln L)^{\beta}$. Analytic arguments place approximate bounds on α and β, as given in Eq. (3) of the paper. Numerical simulations in two dimensions indicate that $\alpha \approx \beta \approx 1$.

(2) The probability of finding the bond with the largest current near the free surfaces of the network is much larger than that of finding the largest current in the bulk. This is quantified by the ratio

$$R = P_{\text{surface}} / P_{\text{bulk}}$$
$$\sim L^{x} .$$

Numerical simulations suggest $x = 0.30 \pm 0.05$ at $p = 0.90$ in two dimensions.

The methods and results of this paper can be used to study many other network models of breakdown, particularly, the brittle fracture and dielectric networks described in Appendix C of our previous paper.[4]

ACKNOWLEDGMENTS

We thank P. D. Beale for useful discussions, the Michigan State University Center for Fundamental Materials Research for financial support, and the National Science Foundation for computer time on the JVNC CYBER205 at Princeton.

APPENDIX: USE OF THE COMPLEX MAPPING METHOD FOR SOLVING TIP ENHANCEMENT PROBLEMS

In the complex mapping method, we can find the required electric potential solution to Laplace's equation in two dimensions from the complex potential function ω defined by

$$\omega = u + iv \; . \tag{A1}$$

The electric field is also cast into a complex form as

$$E = E_x + iE_y = -\frac{\partial u}{\partial x} - i\frac{\partial u}{\partial y} \; .$$

Via Cauchy's relation, this becomes

$$E = E_x + iE_y = -\frac{\partial u}{\partial x} + i\frac{\partial v}{\partial x} \; , \tag{A2}$$

and so the complex electric field is found from the complex potential from the equation

$$E = -\overline{\frac{dw}{dz}} \; , \tag{A3}$$

where $z = x + iy$. It is straightforward then to find the physical electric fields E_x and E_y from the complex electric field E. Now if we assume that $w(z)$ is analytic, u and v in Eq. (A1) obey Laplace's equation. Under a conformal transformation, the transformed u and v again obey Laplace's equation, and we look for conformal transformations that simplify the geometry of the original problem.

We first illustrate the process with a single crack of infinitesimal thickness as depicted in Fig. 9(a). In this figure the electric potential at infinity is linearly increasing with the vertical direction, and has no dependence on the horizontal direction. It is very easy to solve this one-crack problem by the mapping method. We can use the following mapping,

$$\xi = (z^2 - a^2)^{1/2} \; , \tag{A4}$$

to transform the z plane to the ξ plane as shown in Fig. 9(b) where the slit is transformed to an orientation parallel to the external field. The boundary conditions at infinity are unaltered in the transformation, and so the solution in the presense of the transformed slit is trivial provided the slit is of infinitesimal thickness. We then see that in the ξ plane the complex potential is

$$w(\xi) = -iV_0 \xi \; , \tag{A5}$$

which, using (A3), gives the correct solution in the transformed space. This solution in the ξ space is then

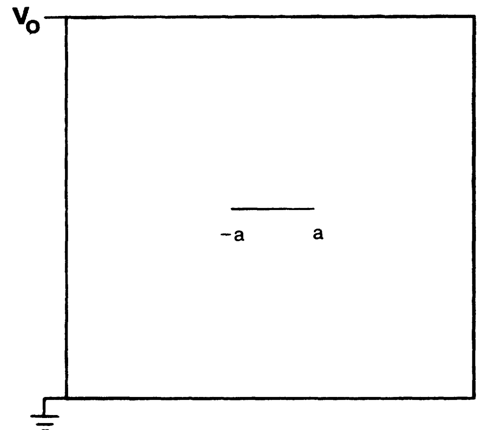

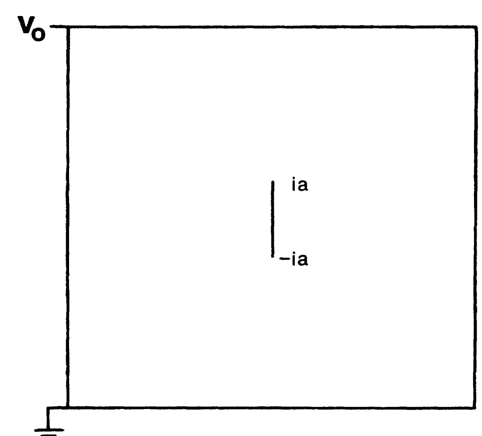

FIG. 9. The single-slit representation of the defect in Fig. 1(a). (a) is the original geometry; (b) is the geometry after conformal transformation. In this geometry the solution is trivial provided the slit has infinitesimal thickness.

transformed back to the z space to find the required solution

$$u+iv=-iV_0[(z^2-a^2)^{1/2}] , \tag{A6}$$

and so, from Eq. (A3), we find

$$E_x-iE_y=iV_0 z/(z^2-a^2)^{1/2} \tag{A7}$$

$$=iV_0(x+iy)/(x^2-y^2-a^2+2ixy)^{1/2} . \tag{A8}$$

On the x axis, $y=0$, the complex electric field becomes

$$E_x-iE_y=iV_0 x/(x^2-a^2)^{1/2} . \tag{A9}$$

As a function of distance (in the x direction along the $y=0$ line) from the defect tip, the electric field is

$$E_y=\pm V_0 x/(x^2-a^2)^{1/2} . \tag{A10}$$

It is interesting to note that E_y and hence the current density in the y direction is singular at the defect tip, in contrast to the ellipse result where the current density is finite at the ellipse tip ($x=a$). However, the two types of continuum defects give the same result in the lattice limit for large system sizes,, as may be seen by integrating the result (A10) over the lattice spacing d:

$$I_{\text{slit}}=j_\infty(2ad+d^2)^{1/2} , \tag{A11}$$

and, taking the large-(a/d) limit, this gives

$$I_{\text{slit}}\sim I_\infty(2a/d)^{1/2} , \tag{A12}$$

which is the same in the large-(a/d) limit as the ellipse result (7) quoted in the text.

We now illustrate how to use this method to solve the two-slit problem depicted in Fig. 2(b). The algebra is quite detailed, so we have included only a few of the intermediate steps. For a full exposition, we refer the reader to Ref. 7. First, make a transformation

$$z=\frac{x+iy}{a+b} , \tag{A13}$$

where a and b are defined in Fig. 2(b), and define

$$k=a/(a+b) . \tag{A14}$$

Now, make the mapping,

$$\xi=i\int_0^z(z^2-\lambda^2)/[(z^2-1)(z^2-k^2)]^{1/2}dz . \tag{A15}$$

This mapping transforms the two-collinear-crack problem of Fig. 2(b) into the "biplane" configuration of Fig. 2(c). The boundary conditions are unaltered in this transformation, except for a rotation by 90°, and in the new geometry the potential in the transformed space is again trivial for infinitesimally thin cracks. We can find the positions of the "biplanes" from the mapping equation (A15),

$$c=\int_k^\lambda(\lambda^2-z^2)/[(1-z^2)(z^2-k^2)]dz \tag{A16}$$

and

$$h=\int_0^k(\lambda^2-z^2)/[(1-z^2)(k^2-z^2)]dz \tag{A17}$$

where c and h are as defined in Fig. 2(c). λ is fixed by the requirement that the mapping (A15) should be independent of path, i.e.,

$$I=\int_C(z^2-\lambda^2)/[(1-z^2)(z^2-k^2)]^{1/2}dz=0 , \tag{A18}$$

where the integral path C includes each of the cracks. Thus,

$$I=2\int_k^1(z^2-\lambda^2)/[(1-z^2)(z^2-k^2)]^{1/2}dz=0 , \tag{A19}$$

i.e.,

$$\int_k^1 z^2/[(1-z^2)(z^2-k^2)]^{1/2}dz=\lambda^2\int_k^1[(1-z^2)(z^2-k^2)]^{-1/2}dz . \tag{A20}$$

Let $z=[1-(1-k^2)u^2]^{1/2}$ and $k'^2=1-k^2$; then,

$$\lambda^2=E(k')/K(k') , \tag{A21}$$

where $K(k)$ and $E(k)$ are elliptic integrals of the first and second kind, respectively. In the ξ plane, we know the complex potential function is simply

$$\omega(\xi)=-V_0\xi . \tag{A22}$$

So, in the z plane, the potential is

$$\omega(z)=-iV_0\int_0^z(z^2-\lambda^2)dz/[(z^2-1)(z^2-k^2)]^{1/2} , \tag{A23}$$

and, from Eq. (A3), we get

$$E_x-iE_y=iV_0(z^2-\lambda^2)/[(z^2-1)(z^2-k^2)]^{1/2} . \tag{A24}$$

On the x axis, we then have

$$E_x-iE_y=-iV_0[x^2-\lambda^2(a+b)^2]/\{[x^2-(a+b)^2](x^2-a^2)\}^{1/2} , \tag{A25}$$

and hence the behavior of the physical electric fields is

$$E_x=0,\quad E_y=\pm V_0[x^2-\lambda^2(a+b)^2]/\{[x^2-(a+b)^2](x^2-a^2)\}^{1/2}\quad(-a<x<a) , \tag{A26}$$

$$E_x=0,\quad E_y=\pm V_0[x^2-\lambda^2(a+b)^2]/\{[x^2-(a+b)^2](x^2-a^2)\}^{1/2}\quad(|x|>a+b) , \tag{A27}$$

$$E_x=\pm V_0[x^2-\lambda^2(a+b)^2]/\{[(a+b)^2-x^2](x^2-a^2)\}^{1/2},\quad E_y=0\quad(a<|x|<a+b) . \tag{A28}$$

To find the current between the two cracks, we integrate Eq. (A26).

$$I_{\text{slits}}=\pm 2V_0\Sigma\int_0^a dx[x^2-\lambda^2(a+b)^2]/\{[x^2-(a+b)^2](x^2-a^2)\}^{1/2} \tag{A29}$$

$$=2V_0\Sigma(a+b)[E(k)-K(k)+E(k')K(k)/K(k')] , \tag{A30}$$

where Σ is the conductance of the system. We are interested in the limit $a \ll b$, which implies $k \to 0$. In this case,

$$I_{\text{slits}} \to 2V_0\Sigma(a+b)E(k')K(k)/K(k') \ . \tag{A31}$$

As $k \to 0$ $k' \to 1$ and $E(k') \to 1$, $E(k) \sim K(k)$ and both are finite, and $K(k')$ is singular.

Because $K(k')$ is singular as $-\ln(1-k'^2)$, we find

$$I_{\text{slits}} \sim V_0\Sigma(a+b)E(k')K(k)/\ln[(a+b)/a] \ , \tag{A32}$$

which is the result quoted in Eq. (14) of the main part of the paper.

To make contact with the result for one slit when the distance between the two slits is zero, take the limit $a \to 0$; then $\lambda^2 = E(k')/K(k') \to 0$, and Eq. (A27) becomes

$$E_y = -V_0 x/(x^2-b^2)^{1/2} \quad \text{for } |x| \geq b \ , \tag{A33}$$

which is the one-crack result reported in Eq. (A10).

[1]S. Kirkpatrick Rev. Mod. Phys. **45**, 574 (1973). D. Stauffer, *Introduction to Percolation Theory* (Taylor and Francis, London, 1985).

[2]L. de Arcangelis, S. Redner, and H. J. Herrmann, J. Phys. (Paris) Lett. **46**, L585 (1985).

[3]P. M. Duxbury, P. D. Beale, and P. L. Leath, Phys. Rev. Lett. **57**, 1052 (1986); **59**, 155(E) (1987).

[4]P. M. Duxbury, P. L. Leath, and P. D. Beale Phys. Rev. B **36**, 367 (1987).

[5]J. Machta and R. A. Guyer, Phys. Rev. B **36**, 2142 (1987).

[6]G. Arfken, *Mathematical Methods for Physicists,* 2nd ed. (Academic, New York, 1970).

[7]G. C. Sih, *Method of Analysis and Solution of Crack Problems* (Noordhoff, Amsterdam, 1973); O. L. Bowie, *ibid.*, and references therein.

[8]E. J. Gumbel, *Statistics of Extremes* (Columbia University Press, New York, 1958).